

Genotype-targeted local therapy of glioma

Ganesh M. Shankar^{a,1}, Ameya R. Kirtane^{b,c,1}, Julie J. Miller^d, Hormoz Mazdiyasi^{b,c}, Jaimie Rogner^{b,c}, Tammy Tai^{b,c}, Erik A. Williams^e, Fumi Higuchi^a, Tareq A. Juratli^a, Kensuke Tateishi^f, Mara V. A. Koerner^a, Shilpa S. Tummala^a, Alexandria L. Fink^a, Tristan Penson^a, Stephen P. Schmidt^g, Gregory R. Wojtkiewicz^g, Aymen Baig^e, Joshua M. Francis^{h,i}, Mikael L. Rinne^{h,i}, Julie M. Batten^e, Tracy T. Batchelor^d, Priscilla K. Brastianos^d, William T. Curry Jr.^a, Fred G. Barker II^a, Justin T. Jordan^d, A. John Iafrate^e, Andrew S. Chiⁱ, Jochen K. Lennerz^e, Matthew Meyerson^{h,i}, Robert Langer^{b,c,2}, Hiroaki Wakimoto^a, Giovanni Traverso^{b,c,k,2}, and Daniel P. Cahill^{a,2}

^aDepartment of Neurosurgery, Massachusetts General Hospital, Harvard Medical School, Boston, MA 02114; ^bDepartment of Chemical Engineering, Massachusetts Institute of Technology, Cambridge, MA 02139; ^cKoch Institute for Integrative Cancer Research, Massachusetts Institute of Technology, Cambridge, MA 02139; ^dStephen E. and Catherine Pappas Center for Neuro-Oncology, Division of Hematology/Oncology, Department of Neurology, Massachusetts General Hospital, Boston, MA 02114; ^eDepartment of Pathology, Massachusetts General Hospital, Boston, MA 02114; ^fDepartment of Neurosurgery, Yokohama City University, Yokohama, Kanagawa Prefecture, Japan 236-0027; ^gCenter for Systems Biology, Massachusetts General Hospital, Boston, MA 02114; ^hDepartment of Medical Oncology, Dana-Farber Cancer Institute, Boston MA 02215; ⁱCancer Program, Broad Institute, Cambridge MA 02142; ^jLaura and Isaac Perlmutter Cancer Center, New York University School of Medicine and New York University Langone Health, New York, NY 10016; and ^kDivision of Gastroenterology, Brigham and Women's Hospital, Harvard Medical School, Boston, MA 02115

Contributed by Robert Langer, July 2, 2018 (sent for review April 6, 2018; reviewed by Gregory J. Riggins and Michael A. Vogelbaum)

Aggressive neurosurgical resection to achieve sustained local control is essential for prolonging survival in patients with lower-grade glioma. However, progression in many of these patients is characterized by local regrowth. Most lower-grade gliomas harbor isocitrate dehydrogenase 1 (*IDH1*) or *IDH2* mutations, which sensitize to metabolism-altering agents. To improve local control of *IDH* mutant gliomas while avoiding systemic toxicity associated with metabolic therapies, we developed a precision intraoperative treatment that couples a rapid multiplexed genotyping tool with a sustained release microparticle (MP) drug delivery system containing an *IDH*-directed nicotinamide phosphoribosyltransferase (NAMPT) inhibitor (GMX-1778). We validated our genetic diagnostic tool on clinically annotated tumor specimens. GMX-1778 MPs showed mutant *IDH* genotype-specific toxicity in vitro and in vivo, inducing regression of orthotopic *IDH* mutant glioma murine models. Our strategy enables immediate intraoperative genotyping and local application of a genotype-specific treatment in surgical scenarios where local tumor control is paramount and systemic toxicity is therapeutically limiting.

intraoperative diagnostics | local therapy | glioma | metabolic therapeutics

Genotype-based therapeutics continue to transform medical oncology. As the most common intrinsic CNS tumor, adult diffuse gliomas hold particular promise for genotype-targeted therapy, since greater than 90% harbor recurrent hotspot mutations within just a few genes: the metabolic enzyme isocitrate dehydrogenase 1 (*IDH1*) or its homolog *IDH2* (1), the telomerase reverse transcriptase (*TERT*) promoter (2), histone H3.3 (*H3F3A*) (3), and signaling kinase *BRAF* (4). However, genotype-targeted therapy has had limited success in CNS tumors, often due to inadequate drug penetration across the blood–brain barrier (BBB) and the resulting nonneurologic toxicities that occur when systemically administered therapeutics are dose increased.

Systemic genotoxic therapeutics display an aggregate survival benefit in large cohorts of patients with *IDH* mutant glioma (5, 6), although potentially at the cost of accelerated mutagenesis and malignant progression in a subset of cases (7). Recently, we and others have reported several alternative pharmacologic approaches to selectively target *IDH1* mutant gliomas (8–11). In particular, we discovered a marked susceptibility of *IDH1* mutant cancers to depletion of NAD⁺ using small molecule inhibitors targeting nicotinamide phosphoribosyltransferase (12). Unlike traditional genotoxic chemotherapeutics, nicotinamide phosphoribosyltransferase inhibitor (NAMPTi) can drive selective cell kill without an antecedent requirement for DNA damage and cell cycle replication, an especially useful feature to target the indolent phase of lower-grade glioma. However, systemic administration of NAMPTi in patients has been

hampered by unfavorable pharmacokinetic properties and dose-limiting hematologic and gastrointestinal toxicities (13).

We and others have reported preoperative (14–18) and intraoperative (19, 20) methods for unambiguous diagnostic identification of *IDH* mutant glioma. With the acceleration of molecular information into the perioperative setting, these techniques could then be coupled with local therapeutic application during a tumor resection. We hypothesized that *IDH* mutant gliomas could benefit from genotype-based surgical therapy with in situ administration of targeted therapies that cannot otherwise be effectively dosed systemically.

Significance

Lower-grade gliomas are often characterized by mutations in metabolism-related genes isocitrate dehydrogenase 1 (*IDH1*) and *IDH2*. Resection of these tumors is constrained by adjacent eloquent cortex, resulting in local failures. Studies showed that *IDH* mutant cells are sensitive to metabolic therapeutics, but these drugs are limited by systemic toxicities. We hypothesized that application of metabolism-altering therapeutics at the surgical margin would improve tumor control and minimize toxicity. We developed an intraoperative diagnostic assay to identify *IDH* mutations. We show that intratumoral administration of sustained release formulations of metabolism-altering compound prolongs survival in a mouse model of *IDH* mutant glioma. This genotype-based paradigm introduces a workflow in surgical oncology that can be extended to other tumors characterized by targetable molecular alterations.

Author contributions: G.M.S., A.R.K., R.L., G.T., and D.P.C. designed research; G.M.S., A.R.K., H.M., J.R., T.T., E.A.W., F.H., T.A.J., K.T., M.V.A.K., S.S.T., A.L.F., T.P., S.P.S., G.R.W., A.B., J.M.B., H.W., G.T., and D.P.C. performed research; G.M.S., A.R.K., J.J.M., H.M., T.A.J., J.M.F., M.L.R., T.T.B., P.K.B., W.T.C., F.G.B., J.T.J., A.J.I., A.S.C., J.K.L., M.M., R.L., H.W., G.T., and D.P.C. analyzed data; and G.M.S., A.R.K., J.J.M., H.M., J.R., T.T., E.A.W., F.H., T.A.J., K.T., M.V.A.K., S.S.T., A.L.F., T.P., S.P.S., G.R.W., A.B., J.M.F., M.L.R., J.M.B., T.T.B., P.K.B., W.T.C., F.G.B., J.T.J., A.J.I., A.S.C., J.K.L., M.M., R.L., H.W., G.T., and D.P.C. wrote the paper.

Reviewers: G.J.R., Johns Hopkins University School of Medicine; and M.A.V., Cleveland Clinic.

Conflict of interest statement: G.M.S., A.R.K., R.L., G.T., and D.P.C. have filed a provisional patent application for this technology.

Published under the PNAS license.

See Commentary on page 8846.

¹G.M.S. and A.R.K. contributed equally to this work.

²To whom correspondence may be addressed. Email: rlanger@mit.edu, ctraverso@bwh.harvard.edu, or cahill@mgh.harvard.edu.

This article contains supporting information online at www.pnas.org/lookup/suppl/doi:10.1073/pnas.1805751115/-DCSupplemental.

Published online August 6, 2018.

Results

Diffuse Astrocytoma Progression Is Predominantly Local Failure. We first characterized the patterns of *IDH* mutant glioma progression (Fig. 1A) by retrospectively analyzing an institutional cohort of 130 patients who underwent resection. We found that 82% experienced tumor regrowth within 2 cm of the initial tumor margin (Fig. 1B). This local failure was a harbinger of poor prognosis, with these patients displaying a shorter progression-free survival in comparison with those experiencing a more distal failure (Fig. 1C). More extensive resection and adjuvant radiation therapy prolonged time to local failure (*SI Appendix*, Fig. S1A), while distal failure did not correlate with extent of resection or administration of adjuvant chemotherapy or radiation therapy (*SI Appendix*, Fig. S1B). Given the pattern of local failure in *IDH* mutant glioma, we hypothesized that the clinical benefit of extensive resection and adjuvant radiation therapy could be augmented by NAMPTi if applied at the tumor margin. The necessary elements of a surgical workflow for precision intraoperative local therapy include rapid and accurate molecular diagnosis combined with delivery of a therapeutic agent at the resection margin (Fig. 2). In this study, we sought to develop a rapid molecular diagnostic and a sustained release formulation of NAMPTi as a prototype for this proposed surgical oncology paradigm.

Formulation of Sustained Release Microparticles of Metabolic Inhibitors

Targeting *IDH* Mutant Glioma. The utility of local chemotherapy for glioma is well-established (21, 22). We extended these prior efforts with the design of a sustained release microparticle (MP) for local delivery of NAMPTi to sensitive tumor types. To establish pharmacokinetic parameters of the drug, we first tested the blood and brain tissue concentrations of GMX-1778, an NAMPTi with partial BBB permeability that is effective in *IDH1* mutant orthotopic glioma xenograft models (12), when administered at known therapeutic doses in nontumor-bearing 6- to 7-wk-old SCID mice. After a single oral dose of 250 mg/kg, GMX-1778 levels reached a peak concentration of $18.0 \pm 3.6 \mu\text{M}$ in the plasma and $3.0 \pm 1.5 \mu\text{M}$ in the brain within 2 h. Within

24 h, GMX-1778 was no longer detectable in brain, indicating that repeated dosing would be required to maintain a therapeutic intracerebral concentration (*SI Appendix*, Fig. S2A). This observation is echoed in clinical trials that find that 1-d-long dosing regimens or intermittent drug holidays result in minimal therapeutic activity (23–25). To ensure consistent therapeutic drug levels, we carried out our toxicity studies using a repeat dosing strategy. Systemic toxicity in nontumor-bearing SCID mice was assessed after dosing GMX-1778 daily for 5 consecutive days. GMX-1778-treated animals had weight loss, while vehicle-treated animals maintained their weight (*SI Appendix*, Fig. S2B) ($17.9 \pm 1.1 \text{ g}$, $n = 5$ vs. $21.8 \pm 0.6 \text{ g}$, $n = 9$ control dextrose-treated animals; $P < 0.05$). GMX-1778-treated animals were also found to have anemia (hemoglobin: $6.7 \pm 0.8 \text{ g/dL}$, $n = 4$ vs. $9.2 \pm 0.5 \text{ g/dL}$, $n = 5$; $P < 0.05$) and uremia ($20.5 \pm 1.9 \text{ mg/dL}$, $n = 4$ vs. $15 \pm 0.5 \text{ mg/dL}$, $n = 4$; $P < 0.05$) (*SI Appendix*, Fig. S2C), and livers examined from killed mice were characterized by eosinophilic cholangitis (*SI Appendix*, Fig. S2D).

For initial MP designs, we opted to encapsulate both GMX-1778 and FK866, a chemically dissimilar but potent NAMPTi that does not measurably accumulate in the brain parenchyma when given systemically, in matrices of poly(lactide-co-glycolide), a well-studied, safe, and biodegradable copolymer. Varying parameters, such as polymer:drug ratio, lactide:glycolide ratio, method of solvent evaporation, and method of mixing (*SI Appendix*, Table S1), we evaluated nine formulations for drug loading and presence of drug crystals by HPLC and SEM, respectively. In some cases, MPs prepared by rapid solvent evaporation were noted to have significant numbers of unbound drug crystals (e.g., Formulation A) (Fig. 3A). These crystals could be removed from the formulation by washing the particles with an ionic surfactant in which drug had high solubility, but this process markedly reduced drug loading [$<0.1\%$ (wt/wt), Formulation H]. Conversely, by washing the particles with nonionic surfactant, we achieved GMX-1778 loading of 4.5% (wt/wt) in a preparation otherwise free of drug crystals (Formulation I) (Fig. 3B). In this formulation, the particle size distribution was unimodal, with peak size measuring between 3 and 4 μm (Fig. 3C). Release

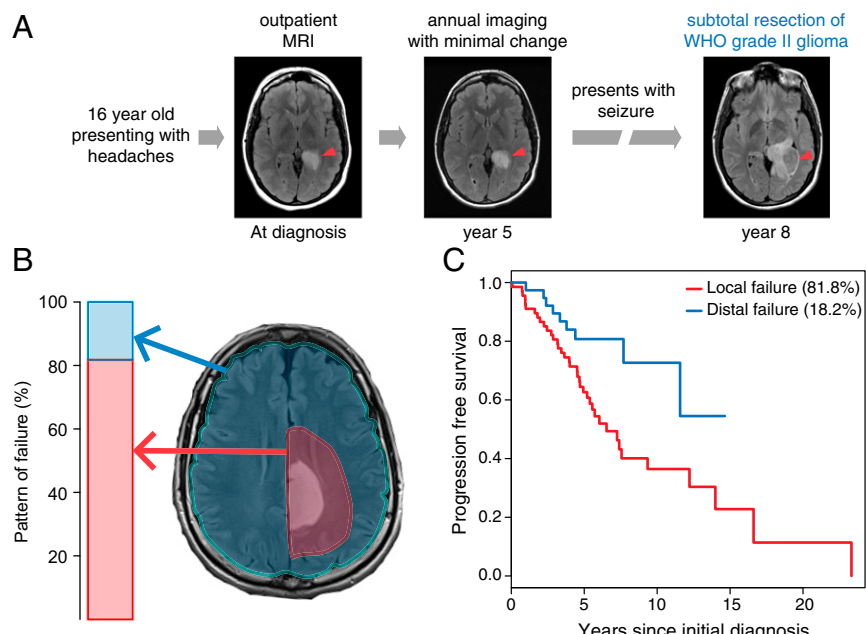


Fig. 1. *IDH1*-mutated diffuse astrocytomas shows local disease progression. (A) This representative patient with diffuse astrocytoma illustrates disease progression adjacent to the initial lesion. (B) Retrospective analysis of 130 patients with *IDH*-mutated diffuse astrocytomas reveals local progression within 2 cm of the initial lesion in 81.8% of patients. (C) Median progression-free survival was 4.7 y for local failure vs. 5.1 y for distal failure.

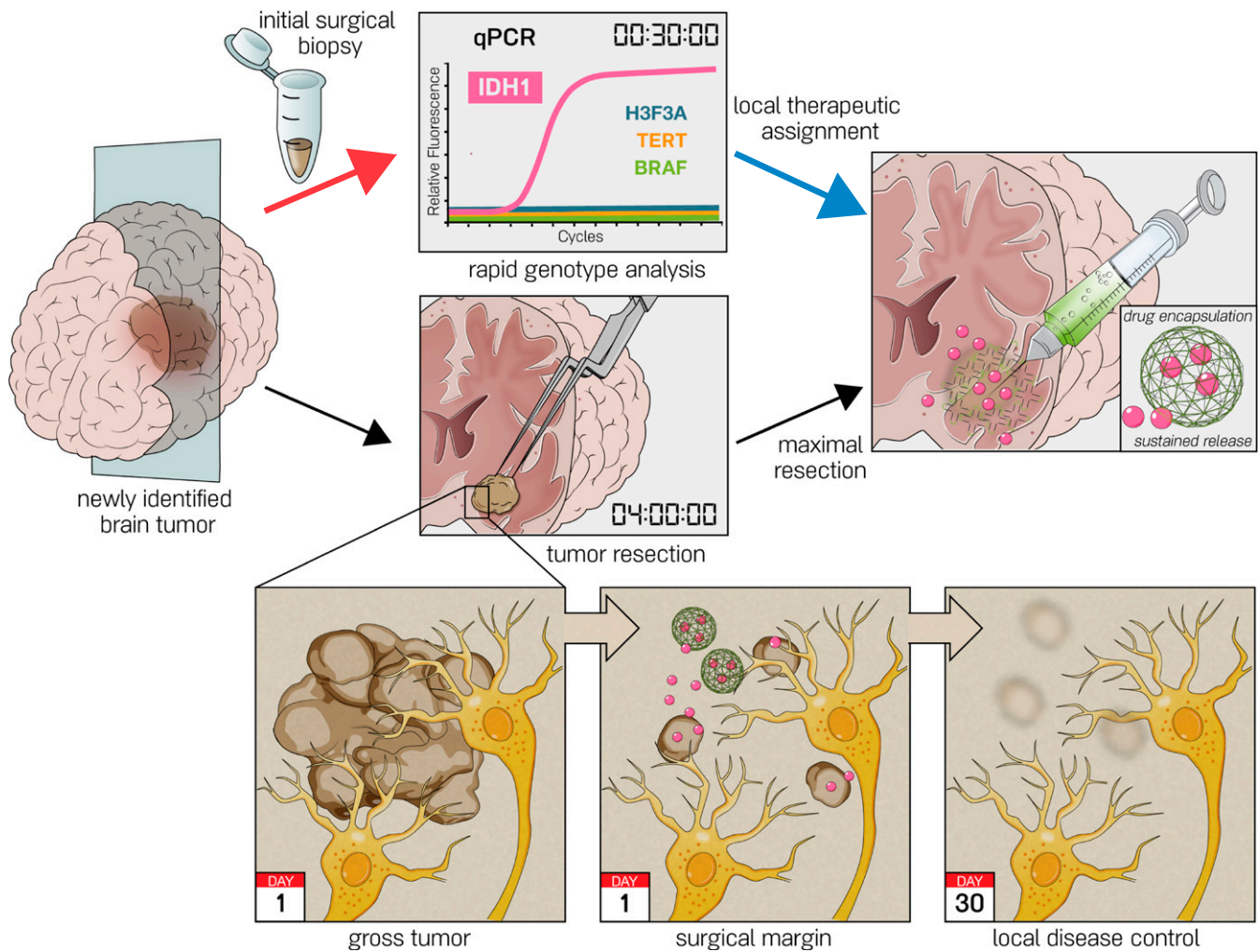


Fig. 2. Proposed intraoperative workflow for genotype-targeted therapy of glioma. Current surgical treatment strategy for patients with nonenhancing brain lesions is maximal resection. Here, we establish a modern paradigm for establishing a molecular diagnosis of a tumor specimen (red arrow) to guide the delivery of a genotype-directed local therapy at the surgical margin during neurosurgical resection (blue arrow) to target the surrounding infiltrative disease (Bottom).

kinetics of this formulation was biphasic, with ~12% released daily for the first 4 d and a cumulative drug release of 60% reached asymptotically after 8 d (Fig. 3D).

In vitro bioactivity assays showed time-dependent decrease in cell viability when GMX-1778 MPs from Formulation I were coincubated with MGG152, an *IDH1* mutant patient-derived glioma line, resulting in a $34.5 \pm 1.7\%$ decrease in viability at 24 h and a $96.3 \pm 0.2\%$ decrease at 72 h (Fig. 3E) ($n = 3$). This effect on cell viability correlated with an on-target pharmacodynamic effect of decreased NAD⁺ levels of $83 \pm 1\%$ at 24 h and $97 \pm 0.1\%$ at 72 h (SI Appendix, Fig. S3A). Similar, although smaller, decreases in cell viability and NAD⁺ levels were noted with an MP formulation using FK866 (Fig. 3E and SI Appendix, Fig. S3A). The effect on cell viability was specific to glioma cells harboring the *IDH1* mutation and not to other *IDH1* wild type, *TERT* promoter-mutated glioma cell lines obtained from tumors of the same histologic grade (Fig. 3F and SI Appendix, Fig. S3B). Analysis of drug concentration in the media revealed a time-dependent increase in GMX-1778 of 40.4 ± 2.3 nM at 24 h and 63.8 ± 3.7 nM at 72 h. Given the more potent activity of GMX-1778 MPs in comparison with FK866 MPs, we opted to pursue the former for subsequent experiments.

Development of Intraoperative Genotyping Diagnostic to Guide Local Targeted Therapy in Glioma. Given this differential response to NAMPTi, we recognized that knowledge of the tumor genetic status is a necessary precursor to administration of precision local therapy (19, 20). To obviate the need for a separate diagnostic procedure and assign genetic status in an intraoperative timeframe, we broadened the diagnostic capability of our previously developed multiplexed qPCR-based rapid genotyping assay (20). By suppressing exponential amplification of wild-type alleles, detection of mutations in *IDH1* at the R132 codon, two *TERT* promoter mutations (C228T and C250T), *H3F3A* at the K27 codon, and *BRAF* at the V600 codon was successful at an allelic fraction of 1% within 27 min (Fig. 4A and SI Appendix, Figs. S4–S7 and Table S2). The detection of *IDH1* R132H in tumor specimens was 100% concordant with immunohistochemistry for the mutant protein; in addition, the genotyping assay was able to capture additional noncanonical *IDH1* mutations that would be otherwise negative by immunohistochemistry (IHC) (Fig. 4B). This sensitivity is within the range of allelic fraction noted in a cohort of infiltrative brain tumor specimens previously analyzed by an orthogonal next generation sequencing assay: *IDH1* R132 mutations median: 32% (5–52%), *TERT* promoter mutation: 23% (12–61%), and *BRAF* V600E: 29% (6–39%) (SI Appendix, Table S3). Detection of one

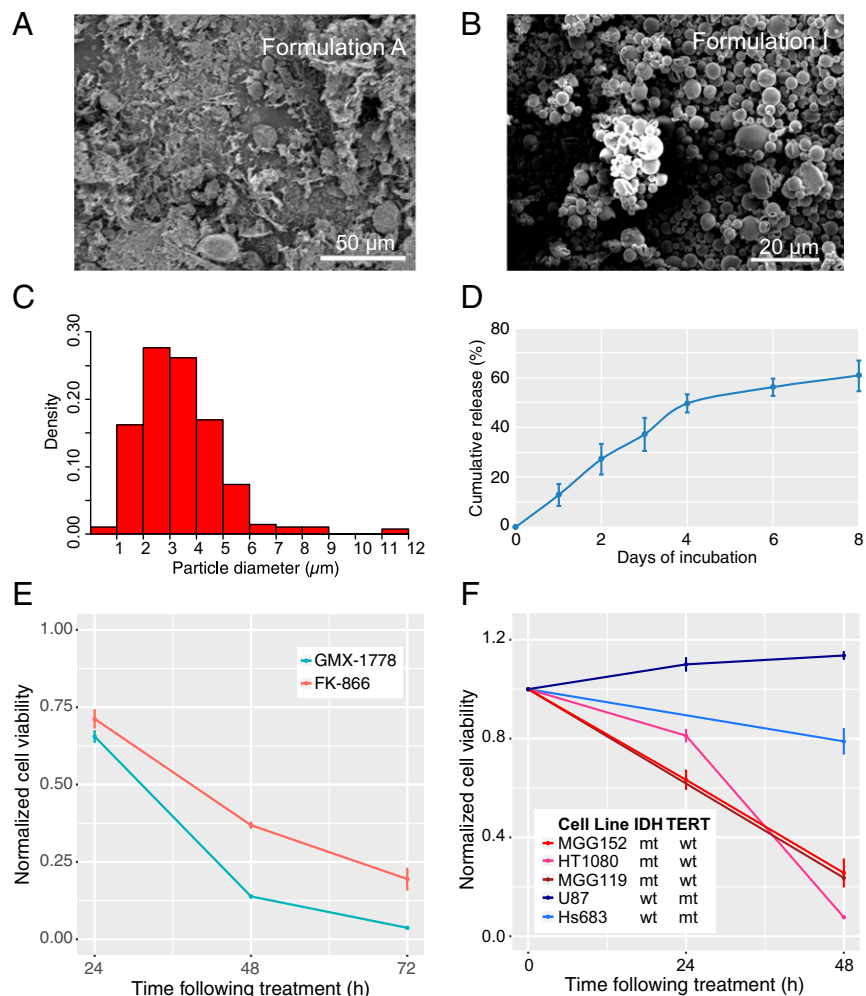


Fig. 3. MP formulation for sustained release of NAMPTis shows selective in vitro activity against IDH-mutated cells. SEM revealed (A) drug crystals in the formulation with highest drug loading and (B) pure MP composition in a formulation with 4.5% drug loading. (C) Mean particle size is $3.4 \pm 1.6 \mu\text{m}$ as measured by SEM imaging followed by processing by ImageJ software. (D) GMX-1778 MPs were dispersed in artificial cerebrospinal fluid and placed at 37°C . At various time points, the particles were separated by centrifugation ($1,500 \times g$ for 10 min). The supernatant was collected for HPLC analysis, and the particles were suspended in fresh release medium. Data are represented as mean \pm SD ($n = 3$). (E) Treatment of MGG152, an IDH1 R132H-mutated human glioma cell line, with MPs containing a total of $1 \mu\text{M}$ GMX-1778 or $1 \mu\text{M}$ FK866 reveals a time-dependent decrease in cell viability compared with cells treated with similarly prepared compound-free MPs over 72 h ($96.3 \pm 0.2\%$ for GMX-1778, $n = 3$ and $80.5 \pm 3.4\%$ for FK866, $n = 3$). HPLC analysis of GMX-1778 in the media of cells treated with the sustained release MP formulation revealed concentrations of $40.4 \pm 2.3 \text{ nM}$ at 24 h and $63.8 \pm 3.7 \text{ nM}$ at 72 h. (F) The time-dependent activity of the GMX-1778 MP formulation was noted in an additional IDH1 R132C-mutated chondrosarcoma cell line HT1080 (red; $n = 3$) and IDH1 R132H-mutated glioma cell line MGG119 (brown) compared with the IDH wild-type glioblastoma cell lines U87 (dark blue; $n = 3$) and Hs683 (light blue; $n = 3$). mt, mutant; wt, wild type.

of the mutations confirmed the presence of tumor tissue, and mutual exclusivity of the alterations served as reciprocal internal positive controls to reserve the intraoperative decision for in situ application of NAMPTi to *IDH* mutant gliomas (26). We validated our assay on 87 clinically annotated brain tumor specimens (Fig. 4B) and found that 75 of 87 brain tumor samples (86%) were captured by the presence of one or more mutations; when restricted to tumors with diffuse glioma histology, >90% of cases are positively assigned. From a tumor diagnostic standpoint, such a high rate of “positive” assignment (vs. assignment by exclusion) allows for confidence to distinguish tumor versus nonneoplastic pathologies.

Metabolic Inhibitor MPs Restrict IDH1 Mutant Glioma Progression. We provisioned our GMX-1778 MPs for use in murine models. Nontumor-bearing mice receiving intracranial injection of GMX-1778 MPs displayed no detectable toxicities. Specifically, no seizures occurred, no local infections occurred, and there was no detectable anemia (hemoglobin: $11.6 \pm 0.4 \text{ g/dL}$ for blank vs. $11.0 \pm 1.1 \text{ g/dL}$ for GMX-1778 MPs). GMX-1778 levels in

brain parenchyma were below the limit of detection by liquid chromatography-mass spectrometry (LC-MS) at 2 or 7 d after intracranial implantation of MPs, consistent with the sustained release of low nanomolar concentrations of compound followed by subsequent clearance.

To then assess whether tumor growth could be impacted *in vivo*, we established orthotopic glioma xenografts by stereotactic intracranial implantation of MGG152 (*IDH1* R132H mutant) or U87 (*IDH* wild type, *TERT* promoter-mutated) cells engineered to express firefly luciferase (SI Appendix, Fig. S8). Established tumor growth was first confirmed by bioluminescence imaging performed 15 d after implantation (Fig. 5A). While the majority of the mass was nodular, these orthotopic tumors also displayed invasive growth (SI Appendix, Fig. S9) similar to the infiltrative histology noted in patients. Notably, a single stereotactic intratumoral injection of GMX-1778 MPs into established tumors resulted in suppression of the MGG152 intracerebral tumor growth compared with stereotactic intratumoral injection of blank MPs (Fig. 5A and B). In accord, intracerebral treatment resulted in a

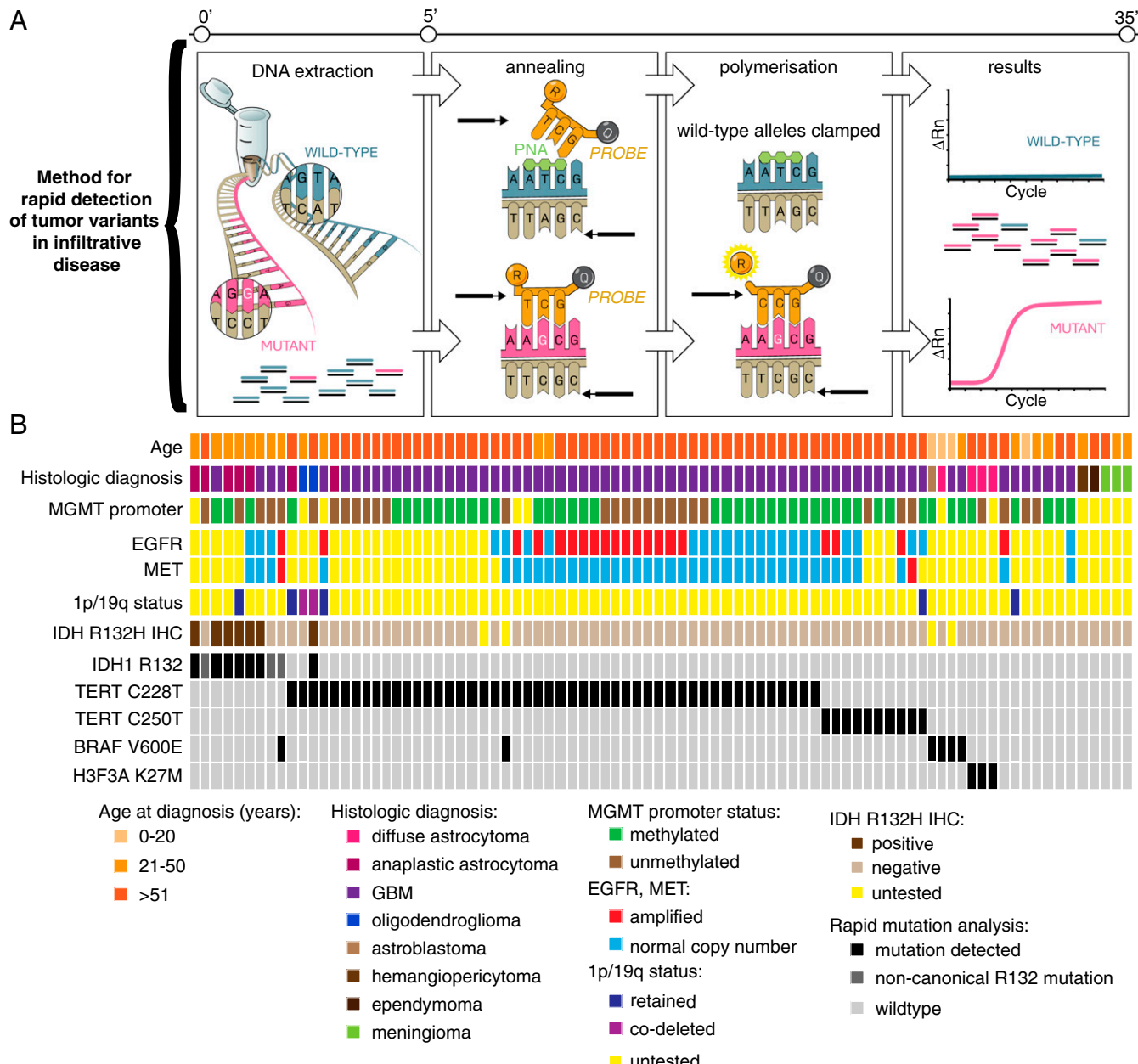


Fig. 4. Method for detection of recurrent mutations noted in glioma allows for rapid molecular genotyping to guide intraoperative decision for use of targeted local therapy. (A) The rapid genotyping assay utilizes Taqman-based probes for fluorescence-based detection of mutant alleles with clamping of the wild-type allele amplicon via peptide nucleic acid oligonucleotides, allowing for detection of tumor variants to an allelic fraction of 1% within 30 min. (B) Validation of genotyping assay correlates mutation call for IDH1 R132, TERT promoter variants, H3F3A K27M, and BRAF V600E in 87 brain tumor specimens from a clinically annotated database. EGFR, epidermal growth factor receptor; GBM, glioblastoma; IHC, immunohistochemistry; MET, tyrosine-protein kinase Met; MGMT, O6-methylguanine DNA methyltransferase; PNA, peptide nucleic acid; Rn, normalized reporter value.

significant improvement in median survival (Fig. 5C) (58.5 ± 3.8 d for blank MPs, $n = 6$ vs. 79.0 ± 3.7 d for GMX-1778 MPs, $n = 8$; $P < 0.01$). As a control, stereotactic intratumoral injection of GMX-1778 MPs did not significantly affect tumor growth or survival in an *IDH* wild-type orthotopic model (Fig. 5A and *SI Appendix*, Fig. S10) (29.5 d for blank MPs, $n = 4$ vs. 29 d for GMX-1778 MPs, $n = 5$).

Discussion

Development of drugs and drug carriers that effectively cross the BBB contributes significantly to our ability to treat brain tumors (27). Since the tumor receives only a small fraction of the blood supply,

drug loss throughout the systemic distribution brings resultant off-target toxicities (28). As such, drug-targeting strategies, such as nanoparticulate carriers and prodrugs, may have the potential to diminish select side effects associated with systemic chemotherapy (29). Surgery uniquely provides direct access to the site of the primary tumor for direct application of sustained release formulations.

Genetically targeted treatment of tumors has had a significant impact on patient survival in many cancer types (30–33). Here, we establish a metabolic local therapy for gliomas that can be integrated into precision surgical oncology workflows. The pursuit of wide marginal resection of the infiltrative borders surrounding *IDH* mutant gliomas (34–37) is constrained by the need to preserve

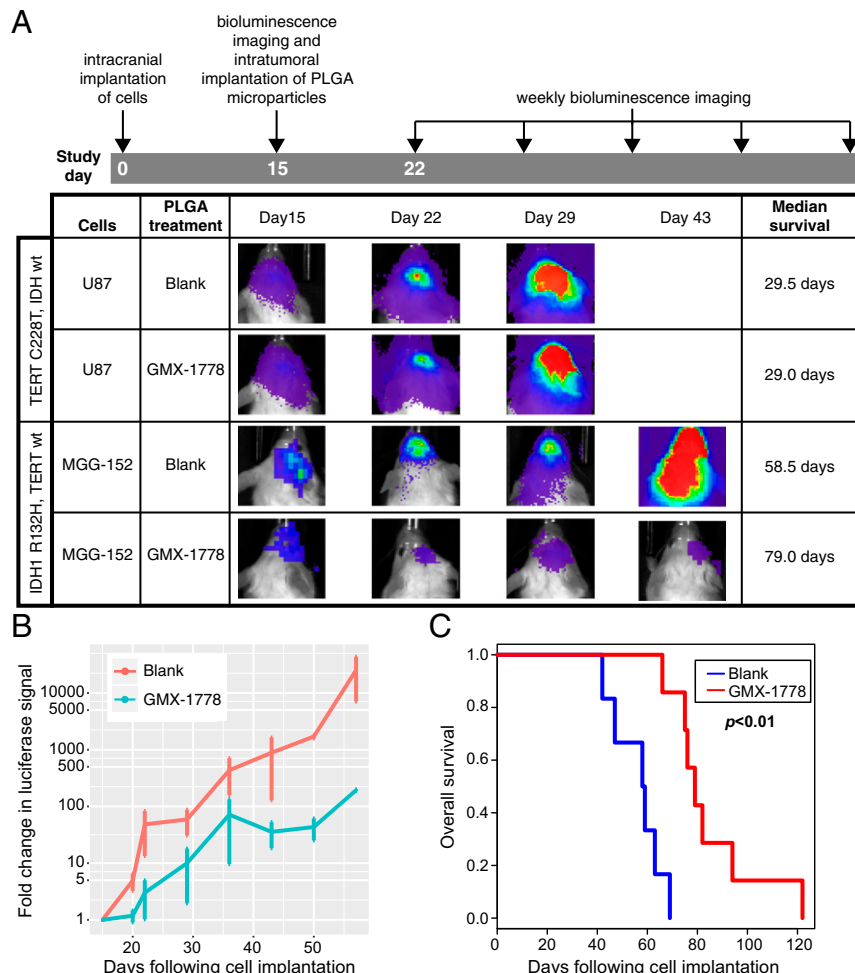


Fig. 5. Intratumoral implantation of sustained release MP formulation shows in vivo activity and increased survival in IDH-mutated orthotopic model. (A) To assess in vivo activity of MP formulation, U87- or MGG152-expressing luciferase (2×10^5 cells) was intracerebrally implanted in SCID mice. Bioluminescence imaging was performed 15 d after implantation to establish a baseline. MPs containing a mass of GMX-1778 to reach a concentration of 5 μ M in a sphere with radius 2 mm were implanted at that time point. Bioluminescence imaging was performed on a weekly basis. No significant difference in survival was noted with GMX-1778 MP implantation in the IDH wild-type U87 glioblastoma orthotopic model ($n = 4$ for blank and $n = 5$ for GMX-1778 MPs). PLGA, poly(lactide-coglycolide). GMX-1778 MPs (B) significantly decreased tumor growth and (C) increased survival in the orthotopic MGG152 model (58.5 d, $n = 6$ for blank vs. 79.0 d, $n = 8$ for GMX-1778 MPs; $P < 0.01$; Cox proportional hazard ratio). wt, wild type.

adjacent functional brain tissue. *IDH* mutant glioma, therefore, represents an ideal oncologic lesion for development of a local delivery strategy given the potential to meaningfully impact the natural history of local progression by direct application of effective treatment at the initial surgical resection margin. While the in vivo model described in this study is akin to *in situ* implantation after stereotactic biopsy, studies in larger animals will be required to test the efficacy of these MPs in a tumor resection model.

Indeed, further assessments of drug-specific pharmacokinetics of MPs are needed to select the optimal formulation to advance into future clinical trials. For instance, BBB-impermeable compounds, such as FK866, may be more effective when delivered locally. Furthermore, the delayed but inevitable progression in the *IDH* mutant orthotopic model after local delivery of NAMPTi could be related to bioavailability of the drug at the tumor margins or acquired resistance to monotherapy with NAMPTi alone. Given our recent findings of a combination metabolic effect between alkylating chemotherapeutics and NAMPTi in *IDH* mutant cancers (38), synergistic strategies combining local MP administration with standard-of-care systemic temozolomide could further augment therapeutic benefit and potentially minimize the development of resistant escape clones.

More generally, NAMPTi sustained release MPs could find utility for local metabolic treatment of other tumors characterized by *IDH1* mutation, such as cholangiocarcinoma (39) or cartilaginous tumors (40–42). Within the CNS, the pairing of intraoperative molecular diagnosis with local targeted therapy could also be pursued for other tumors bearing hotspot mutations captured on our diagnostic platform, such as *BRAF* mutant gliomas, melanoma brain metastases, or craniopharyngiomas (43, 44). Additionally, application of precision therapies locally represents an opportunity for the reconsideration of otherwise effective anticancer agents that have been abandoned due to systemic toxicities. Approaches similar to our strategy could enable genotype-based local therapeutics for other genetically defined cancers during surgical intervention.

Materials and Methods

Clinical and radiographic retrospective review was performed under institutional review board protocols at Massachusetts General Hospital and University Hospital Dresden, with an approved waiver of consent. An intraoperative genotyping assay was engineered to be sensitive to diagnostic hotspot mutations in *IDH1* R132, *TERT* promoter, *H3F3A* K28M, or *BRAF* V600E at 1% allelic fraction and validated on clinically annotated CNS specimens. Biodegradable MPs containing *IDH1*-directed NAMPTis were designed to provide sustained local delivery of

these compounds. MPs were tested for in vitro activity in cell culture and in vivo efficacy in murine orthotopic *IDH1* mutant glioma models (*SI Appendix, SI Materials and Methods*).

ACKNOWLEDGMENTS. We thank Ania Hupalowska for assistance with illustrations. This work is supported in part by the American Brain Tumor Association

Basic Research Fellowship (to G.M.S.) supported by the Humor to Fight the Tumor Committee; NIH Grant EB000244 (to A.R.K. and G.T.); the Division of Gastroenterology, Brigham and Women's Hospital (G.T.); NIH Specialized Programs of Research Excellence (SPORE) Grant P50CA165962 (to D.P.C.); Burroughs Wellcome Career Award in the Medical Sciences 1007616.02 (to D.P.C.); and NIH Grant R01CA227821 (to D.P.C.).

1. Balss J, et al. (2008) Analysis of the *IDH1* codon 132 mutation in brain tumors. *Acta Neuropathol* 116:597–602.
2. Killela PJ, et al. (2013) TERT promoter mutations occur frequently in gliomas and a subset of tumors derived from cells with low rates of self-renewal. *Proc Natl Acad Sci USA* 110:6021–6026.
3. Schwartzentruber J, et al. (2012) Driver mutations in histone H3.3 and chromatin remodelling genes in paediatric glioblastoma. *Nature* 482:226–231.
4. Schindler G, et al. (2011) Analysis of *BRAF* V600E mutation in 1,320 nervous system tumors reveals high mutation frequencies in pleomorphic xanthoastrocytoma, ganglioglioma and extra-cerebellar pilocytic astrocytoma. *Acta Neuropathol* 121:397–405.
5. Cairncross JG, et al. (2014) Benefit from procarbazine, lomustine, and vincristine in oligodendroglial tumors is associated with mutation of *IDH1*. *J Clin Oncol* 32:783–790.
6. Buckner JC, et al. (2016) Radiation plus procarbazine, CCNU, and vincristine in low-grade glioma. *N Engl J Med* 374:1344–1355.
7. Johnson BE, et al. (2014) Mutational analysis reveals the origin and therapy-driven evolution of recurrent glioma. *Science* 343:189–193.
8. Seltzer MJ, et al. (2010) Inhibition of glutaminase preferentially slows growth of glioma cells with mutant *IDH1*. *Cancer Res* 70:8981–8987.
9. Rohle D, et al. (2013) An inhibitor of mutant *IDH1* delays growth and promotes differentiation of glioma cells. *Science* 340:626–630.
10. Grassian AR, et al. (2014) *IDH1* mutations alter citric acid cycle metabolism and increase dependence on oxidative mitochondrial metabolism. *Cancer Res* 74:3317–3331.
11. Saha SK, et al. (2016) Isocitrate dehydrogenase mutations confer dasatinib hypersensitivity and SRC dependence in intrahepatic cholangiocarcinoma. *Cancer Discov* 6:727–739.
12. Tateishi K, et al. (2015) Extreme vulnerability of *IDH1* mutant cancers to NAD⁺ depletion. *Cancer Cell* 28:773–784.
13. Sampath D, Zabka TS, Misner DL, O'Brien T, Dragovich PS (2015) Inhibition of nicotinamide phosphoribosyltransferase (NAMPT) as a therapeutic strategy in cancer. *Pharmacol Ther* 151:16–31.
14. Andronesi OC, et al. (2013) Detection of oncogenic *IDH1* mutations using magnetic resonance spectroscopy of 2-hydroxyglutarate. *J Clin Invest* 123:3659–3663.
15. Choi C, et al. (2012) 2-hydroxyglutarate detection by magnetic resonance spectroscopy in *IDH*-mutated patients with gliomas. *Nat Med* 18:624–629.
16. Elkhaled A, et al. (2012) Magnetic resonance of 2-hydroxyglutarate in *IDH1*-mutated low-grade gliomas. *Sci Transl Med* 4:116ra5.
17. Kalinina J, et al. (2012) Detection of “oncometabolite” 2-hydroxyglutarate by magnetic resonance analysis as a biomarker of *IDH1/2* mutations in glioma. *J Mol Med (Berl)* 90:1161–1171.
18. Pope WB, et al. (2012) Non-invasive detection of 2-hydroxyglutarate and other metabolites in *IDH1* mutant glioma patients using magnetic resonance spectroscopy. *J Neurooncol* 107:197–205.
19. Santagata S, et al. (2014) Intraoperative mass spectrometry mapping of an oncometabolite to guide brain tumor surgery. *Proc Natl Acad Sci USA* 111:11121–11126.
20. Shankar GM, et al. (2015) Rapid intraoperative molecular characterization of glioma. *JAMA Oncol* 1:662–667.
21. Brem H, et al.; The Polymer-brain Tumor Treatment Group (1995) Placebo-controlled trial of safety and efficacy of intraoperative controlled delivery by biodegradable polymers of chemotherapy for recurrent gliomas. *Lancet* 345:1008–1012.
22. Moses MA, Brem H, Langer R (2003) Advancing the field of drug delivery: Taking aim at cancer. *Cancer Cell* 4:337–341.
23. Hovstadius P, et al. (2002) A Phase I study of CHS 828 in patients with solid tumor malignancy. *Clin Cancer Res* 8:2843–2850.
24. Ravaud A, et al. (2005) Phase I study and pharmacokinetic of CHS-828, a guanidino-containing compound, administered orally as a single dose every 3 weeks in solid tumours: An ECSG/EORTC study. *Eur J Cancer* 41:702–707.
25. Zabka TS, et al. (2015) Retinal toxicity, in vivo and in vitro, associated with inhibition of nicotinamide phosphoribosyltransferase. *Toxicol Sci* 144:163–172.
26. Aibaudula A, et al. (2017) Adult *IDH* wild-type lower-grade gliomas should be further stratified. *Neuro Oncol* 19:1327–1337.
27. Pardridge WM (2005) The blood-brain barrier: Bottleneck in brain drug development. *NeuroRx* 2:3–14.
28. Siegel RA, Kirtane AR, Panyam J (2017) Assessing the benefits of drug delivery by nanocarriers: A partico/pharmacokinetic framework. *IEEE Trans Biomed Eng* 64:2176–2185.
29. Peer D, et al. (2007) Nanocarriers as an emerging platform for cancer therapy. *Nat Nanotechnol* 2:751–760.
30. Lynch TJ, et al. (2004) Activating mutations in the epidermal growth factor receptor underlying responsiveness of non-small-cell lung cancer to gefitinib. *N Engl J Med* 350:2129–2139.
31. Motzer RJ, et al. (2007) Sunitinib versus interferon alfa in metastatic renal-cell carcinoma. *N Engl J Med* 356:115–124.
32. Hyman DM, et al. (2015) Vemurafenib in multiple nonmelanoma cancers with *BRAF* V600 mutations. *N Engl J Med* 373:726–736.
33. Long GV, et al. (2016) Overall survival and durable responses in patients with *BRAF* V600-mutant metastatic melanoma receiving dabrafenib combined with trametinib. *J Clin Oncol* 34:871–878.
34. Jakola AS, et al. (2012) Comparison of a strategy favoring early surgical resection vs a strategy favoring watchful waiting in low-grade gliomas. *JAMA* 308:1881–1888.
35. Beiko J, et al. (2014) *IDH1* mutant malignant astrocytomas are more amenable to surgical resection and have a survival benefit associated with maximal surgical resection. *Neuro-oncol* 16:81–91.
36. Kawaguchi T, et al. (2016) Impact of gross total resection in patients with WHO grade III glioma harboring the *IDH* 1/2 mutation without the 1p/19q co-deletion. *J Neurooncol* 129:505–514.
37. Wijnenga MMJ, et al. (2018) The impact of surgery in molecularly defined low-grade glioma: An integrated clinical, radiological and molecular analysis. *Neuro Oncol* 20:103–112.
38. Tateishi K, et al. (2017) The alkylating chemotherapeutic temozolomide induces metabolic stress in *IDH1*-mutant cancers and potentiates NAD⁺ depletion-mediated cytotoxicity. *Cancer Res* 77:4102–4115.
39. Farshidfar F, et al.; Cancer Genome Atlas Network (2017) Integrative genomic analysis of cholangiocarcinoma identifies distinct *IDH*-mutant molecular profiles. *Cell Rep* 19:2878–2880.
40. Amary MF, et al. (2011) Ollier disease and Maffucci syndrome are caused by somatic mosaic mutations of *IDH1* and *IDH2*. *Nat Genet* 43:1262–1265.
41. Pansuriya TC, et al. (2011) Somatic mosaic *IDH1* and *IDH2* mutations are associated with enchondroma and spindle cell hemangioma in Ollier disease and Maffucci syndrome. *Nat Genet* 43:1256–1261.
42. Peterse EFP, et al. (2017) NAD synthesis pathway interference is a viable therapeutic strategy for chondrosarcoma. *Mol Cancer Res* 15:1714–1721.
43. Brastianos PK, et al. (2015) Dramatic response of *BRAF* V600E mutant papillary craniopharyngioma to targeted therapy. *J Natl Cancer Inst* 108:djv310.
44. Rostami E, et al. (2017) Recurrent papillary craniopharyngioma with *BRAF*V600E mutation treated with neoadjuvant-targeted therapy. *Acta Neurochir (Wien)* 159:2217–2221.